

A Geometric Form for the Extended Patience Sorting Algorithm

Alexander Burstein

Department of Mathematics
Iowa State University
Ames, IA 50011-2064, USA
`burstein@math.iastate.edu`

Isaiah Lankham*

Department of Mathematics
University of California, Davis
Davis, CA 95616-8633, USA
`issy@math.ucdavis.edu`

Submitted: June 1, 2005

2000 Mathematics Subject Classifications: 05A05, 05A18 (Primary) 05E10 (Secondary)

Abstract

Patience Sorting is a combinatorial algorithm that can be viewed as an iterated, non-recursive form of the Schensted Insertion Algorithm. In recent work the authors extended Patience Sorting to a full bijection between the symmetric group and certain pairs of combinatorial objects that are most naturally defined in terms of generalized permutation pattern and barred pattern avoidance. This Extended Patience Sorting Algorithm is very similar to the Robinson-Schensted-Knuth (or RSK) Correspondence, which is itself built from repeated application of the Schensted Insertion Algorithm.

In this work we introduce a geometric form for the Extended Patience Sorting Algorithm that is in some sense a natural dual algorithm to G. Viennot's celebrated Geometric RSK Algorithm. We then discuss the relationship between this geometric algorithm and generalized permutation patterns.

1 Introduction

The term *Patience Sorting* was introduced in 1962 by C.L. Mallows [7, 8] as the name of a card sorting algorithm invented by A.S.C. Ross. This algorithm works by first partitioning

*The work of the second author was supported in part by the U.S. National Science Foundation under Grants DMS-0135345 and DMS-0304414.

a shuffled deck of n cards (which we take to be a permutation $\sigma \in \mathfrak{S}_n$) into its left-to-right minima subsequences (called *piles* in this context), and the method used to form these piles can be viewed as an iterated, non-recursive form of the Schensted Insertion Algorithm for interposing values into the rows of a Young tableau (see [1] and [3]). For given $\sigma \in \mathfrak{S}_n$, we call the resulting collection of piles (given as part of the more general Algorithm 1.2 below) the *pile configuration* corresponding to σ and denote it by $R(\sigma)$.

Given a pile configuration R , one forms its *reverse patience word* $RPW(R)$ by listing the piles in R “from bottom to top, left to right” (i.e., by reversing the “far-eastern reading”) as illustrated in Example 1.1 below. In recent work [3] the authors used G. Viennot’s (northeast) shadow diagram construction (defined in [10] and summarized in Section 2.1 below) to characterize these words as the elements of the set $S_n(3\bar{1}\text{-}42)$. That is, reverse patience words are exactly those permutations that avoid the generalized permutation pattern 2-31 unless the elements corresponding to this pattern are also contained in a 3-1-42 pattern. (Recall that by default the elements matching a generalized permutation pattern are required to be contiguous unless a dash is inserted between them. See Bóna [2] for more details regarding permutation patterns in general.)

Example 1.1. The permutation $\sigma = 64518723 \in \mathfrak{S}_8$ has pile configuration $R(\sigma) = \{\{6 > 4 > 1\}, \{5 > 2\}, \{8 > 7 > 3\}\}$, which we represent visually as

$$\begin{array}{ccc} 1 & & 3 \\ 4 & 2 & 7 \\ 6 & 5 & 8 \end{array}$$

Furthermore, the reverse patience word for $R(\sigma)$ is $RPW(R(64518723)) = 64152873 \in S_n(3\bar{1}\text{-}42)$.

In [3] the authors also extended the process of forming piles under Patience Sorting so that it essentially becomes a full non-recursive analog of the famous Robinson-Schensted-Knuth (or RSK) Correspondence. As with RSK, this Extended Patience Sorting Algorithm (Algorithm 1.2 below) takes a simple idea (that of placing cards into piles) and uses it to build a bijection between elements of the symmetric group \mathfrak{S}_n and certain pairs of combinatorial objects. In the case of RSK, one uses the Schensted Insertion Algorithm to build a bijection with pairs of standard Young tableau having the same shape (a partition λ of n , denoted $\lambda \vdash n$; see [9]). However, in the case of Patience Sorting, one achieves a bijection between permutations and somewhat more restricted pairs of pile configurations. In particular, these pairs must not only have the same shape (a composition γ of n , denoted $\gamma \circ\text{-} n$) but their reverse patience words must also simultaneously avoid containing a particular pair of generalized permutation patterns in the same positions (see Section 5 below.) This simultaneous pattern avoidance can also be understood using Viennot’s (northeast) shadow diagram construction for the permutation implicitly defined by a pair of pile configurations (see [3] for more details), but it is only really geometrically characterized by Geometric Patience Sorting.

Viennot introduced the shadow diagram of a permutation in the context of studying the Schützenberger Symmetry Property for RSK. Specifically, one can use recursively defined shadow diagrams to construct the RSK Correspondence completely geometrically. We review this process in Section 2 below. Then in Section 3 we define a natural dual to Viennot’s Geometric RSK Algorithm that similarly characterizes the Extended Patience Sorting Algorithm geometrically. Having defined these two algorithms, we then discuss in Section 4 the principal differences between them, and we conclude with how Geometric Patience Sorting is related to generalized permutation patterns and barred pattern avoidance in Section 5.

We close this introduction by stating the Extending Patience Sorting Algorithm and giving an example.

Algorithm 1.2 (Extended Patience Sorting Algorithm). Given a shuffled deck of cards $\sigma = c_1c_2 \cdots c_n$, inductively build *insertion piles* $R = R(\sigma) = \{r_1, r_2, \dots, r_m\}$ and *recording piles* $S = S(\sigma) = \{s_1, s_2, \dots, s_m\}$ as follows:

- Place the first card c_1 from the deck into a pile r_1 by itself, and set $s_1 = \{1\}$.
- For each remaining card c_i ($i = 2, \dots, n$), consider the cards d_1, d_2, \dots, d_k atop the piles r_1, r_2, \dots, r_k that have already been formed.
 - If $c_i > \max\{d_1, d_2, \dots, d_k\}$, then put c_i into a new pile r_{k+1} by itself and set $s_{k+1} = \{i\}$.
 - Otherwise, find the left-most card d_j that is larger than c_i and put the card c_i atop pile r_j while simultaneously putting i at the bottom of pile s_j .

Example 1.3. Let $\sigma = 64518723 \in \mathfrak{S}_8$. Then according to Algorithm 1.2 we simultaneously form the following pile configurations:

	insertion piles	recording piles		insertion piles	recording piles
Form a new pile with 6 :	6	1	Then play the 4 on it:	4 6	1 2
Form a new pile with 5 :	4 6 5	1 2 3	Add the 1 to left pile:	1 4 6 5	1 2 4 3

Form a	1	1	Then	1	1
new pile	4	2	play the	4	7 2 5
with 8 :	6 5 8	4 3 5	7 on it:	6 5 8	4 3 6
Add the	1	1	Add the	1	3 1 5
2 to mid-	4 2 7	2 3 5	3 to right	4 2 7	2 3 6
dle pile:	6 5 8	4 7 6	pile:	6 5 8	4 7 8

The idea behind Algorithm 1.2 is that we are using a new pile configuration $S(\sigma)$ (called the “recording piles”) to implicitly label the order in which the elements of the permutation σ are added to the usual Patience Sorting pile configuration $R(\sigma)$ (which we will now by analogy to RSK also call the “insertion piles”). It is clear that this information then allows us to uniquely reconstruct σ by reversing the order in which the cards were played. However, even though reversing the Extended Patience Sorting Algorithm is much easier than reversing the RSK Algorithm through recursive “reverse row bumping,” the trade-off is that the pairs of pile configurations that result from the Extended Patience Sorting Algorithm are not independent (as is discussed in Section 5 below), whereas the standard Young tableau pairs generated by RSK are completely independent (up to shape).

2 Northeast Shadow Diagrams and Viennot’s Geometric RSK

In this section we briefly develop Viennot’s geometric form for RSK in order to motivate the geometric form for the Extended Patience Sorting that is introduced in Section 3 below.

2.1 The Northeast Shadow Diagram of a Permutation

We begin with the following fundamental definition:

Definition 2.1. Given a lattice point $(m, n) \in \mathbb{Z}^2$, we define the *northeast shadow* of (m, n) to be the quarter space $S_{NE}(m, n) = \{(x, y) \in \mathbb{R}^2 \mid x \geq m, y \geq n\}$.

See Figure 2.1(a) for an example of a point’s northeast shadow.

The most important use of these shadows is in building so-called northeast shadowlines:

Definition 2.2. Given lattice points $(m_1, n_1), (m_2, n_2), \dots, (m_k, n_k) \in \mathbb{Z}^2$, we define their *northeast shadowline* to be the boundary of the union of the northeast shadows $S_{NE}(m_1, n_1), S_{NE}(m_2, n_2), \dots, S_{NE}(m_k, n_k)$.

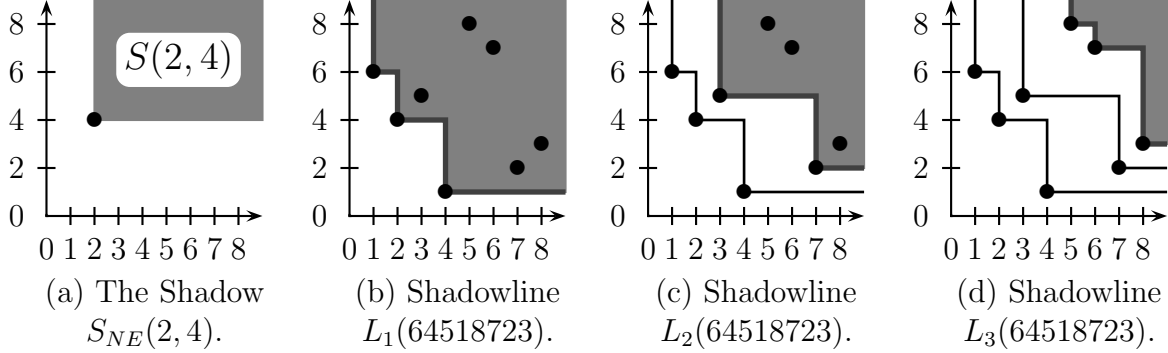


Figure 2.1: Examples of Northeast Shadow and Shadowline Constructions

In particular, we wish to associate to each permutation a certain collection of northeast shadowlines (as illustrated in Figure 2.1(b)–(d)):

Definition 2.3. Given a permutation $\sigma = \sigma_1\sigma_2\cdots\sigma_n \in \mathfrak{S}_n$, the *northeast shadow diagram* $D_{NE}(\sigma)$ of σ consists of the shadowlines $L_1(\sigma), L_2(\sigma), \dots, L_k(\sigma)$ formed as follows:

- $L_1(\sigma)$ is the northeast shadowline for the lattice points $\{(1, \sigma_1), (2, \sigma_2), \dots, (n, \sigma_n)\}$.
- While at least one of the points $(1, \sigma_1), (2, \sigma_2), \dots, (n, \sigma_n)$ is not contained in the shadowlines $L_1(\sigma), L_2(\sigma), \dots, L_j(\sigma)$, define $L_{j+1}(\sigma)$ to be the northeast shadowline for the points

$$\{(i, \sigma_i) \mid (i, \sigma_i) \notin \bigcup_{k=1}^j L_k(\sigma)\}.$$

In other words, we define the shadow diagram inductively by taking $L_1(\sigma)$ to be the shadowline for the diagram $\{(1, \sigma_1), (2, \sigma_2), \dots, (n, \sigma_n)\}$ of the permutation. Then we ignore the points whose shadows were used in building $L_1(\sigma)$ and define $L_2(\sigma)$ to be the shadowline of the resulting subset of the permutation diagram (regardless of which shadowline they lie upon). We then build $L_3(\sigma)$ as the shadowline for the points not yet used in constructing both $L_1(\sigma)$ and $L_2(\sigma)$, and this process continues until all points in the permutation diagram are exhausted.

We can characterize the points whose shadows define the shadowlines at each stage as follows: they are the smallest collection of unused points whose shadows collectively contain all other remaining unused points (and hence the shadows of those points). As a consequence of this shadow containment property, the shadowlines in a northeast shadow diagram will never cross. However, as we will see in Section 3.1 below, the dual construction to Definition 2.3 that is introduced will allow for crossing shadowlines (which are characterized in [4]). The most fundamental cause for this distinction is the way that we will reverse the above shadow containment property for the points used in defining southwest shadowlines.

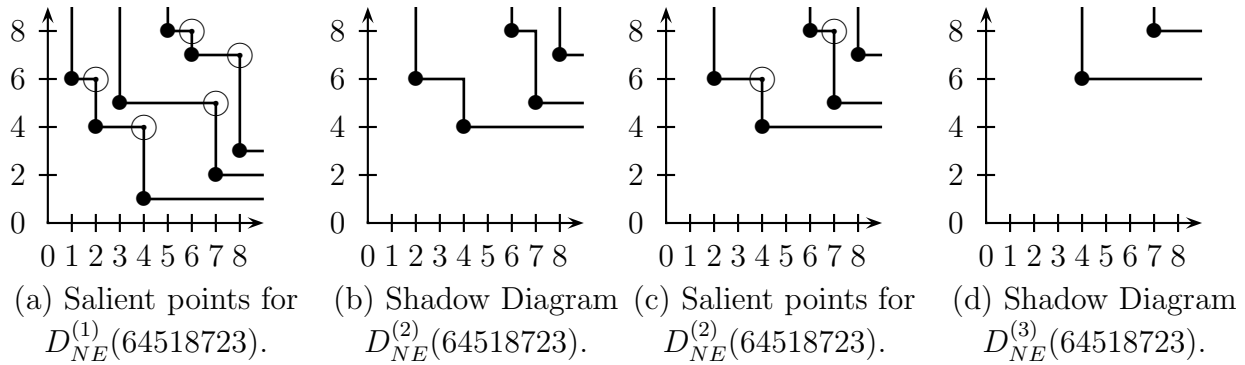


Figure 2.2: The northeast shadow diagrams for 64518723.

2.2 Viennot’s Geometric RSK Algorithm

As simple as northeast shadowlines were to define in the previous section, a great deal of information can still be gotten from them. One of the most basic properties of the northeast shadow diagram $D_{NE}^{(1)}(\sigma) = D_{NE}(\sigma)$ for a permutation $\sigma \in \mathfrak{S}_n$ is that it encodes the top row of the RSK insertion tableau $P(\sigma)$ (resp. recording tableau $Q(\sigma)$) as the smallest ordinates (resp. smallest abscissae) of all points belonging to the constituent shadowlines $L_1(\sigma), L_2(\sigma), \dots, L_k(\sigma)$. One proves this by comparing the use of Schensted Insertion on the top row of the insertion tableau with the intersection of the vertical lines $x = a$. In particular, as a increases from 0 to n , $x = a$ intersects the lattice points in the permutation diagram in the order they are inserted in the top row, and so shadowlines connect elements of σ to those smaller elements that will eventually bump them. (See Sagan [9].)

Remarkably, one can then use the northeast corners (called the *salient points*) of $D_{NE}^{(1)}(\sigma)$ to form a new shadow diagram $D_{NE}^{(2)}(\sigma)$ that similarly gives the second rows of $P(\sigma)$ and $Q(\sigma)$. Then, inductively, the salient points of $D_{NE}^{(2)}(\sigma)$ can be used to give the third rows of $P(\sigma)$ and $Q(\sigma)$, and so on. As such, one can view this recursive formation of shadow diagrams as a geometric form for the RSK correspondence. We illustrate this process in Figure 2.2 for the following permutation from Example 1.3:

$$\sigma = 64518723 \xleftrightarrow{RSK} \left(\begin{array}{|c|c|c|} \hline 1 & 2 & 3 \\ \hline 4 & 5 & 7 \\ \hline 6 & 8 & \\ \hline \end{array}, \begin{array}{|c|c|c|} \hline 1 & 3 & 5 \\ \hline 2 & 6 & 8 \\ \hline 4 & 7 & \\ \hline \end{array} \right)$$

3 Southwest Shadow Diagrams and Geometric Patience Sorting

In this section we introduce a very natural dual algorithm to Viennot’s geometric form for RSK as given in Section 2.2 above.

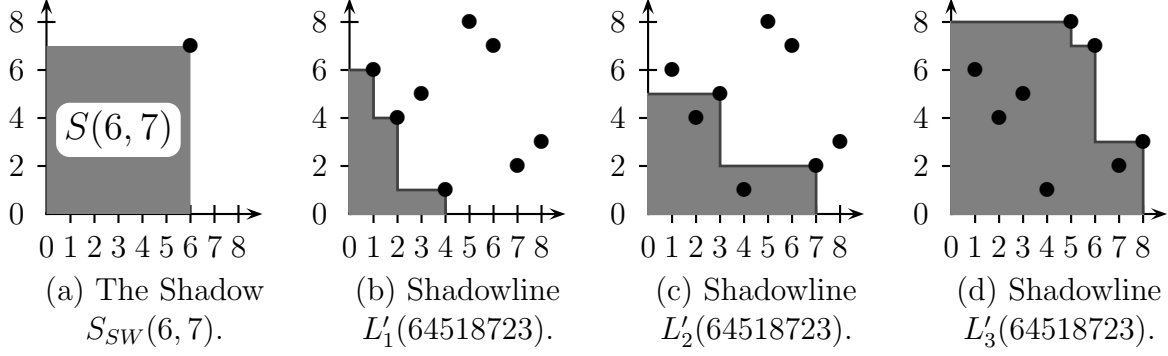


Figure 3.1: Examples of Southwest Shadow and Shadowline Constructions

3.1 The Southwest Shadow Diagram of a Permutation

As in Section 2.1, we begin with the following fundamental definition:

Definition 3.1. Given a lattice point $(m, n) \in \mathbb{Z}^2$, we define the *southwest shadow* of (m, n) to be the quarter space $S_{SW}(m, n) = \{(x, y) \in \mathbb{R}^2 \mid x \leq m, y \leq n\}$.

See Figure 3.1(a) for an example of a point's southwest shadow.

As with their northeast counterparts, the most important use of these shadows is in building southwest shadowlines:

Definition 3.2. Given lattice points $(m_1, n_1), (m_2, n_2), \dots, (m_k, n_k) \in \mathbb{Z}^2$, we define their *southwest shadowline* to be the boundary of the union of the shadows $S_{SW}(m_1, n_1), S_{SW}(m_2, n_2), \dots, S_{SW}(m_k, n_k)$.

In particular, we wish to associate to each permutation a certain collection of southwest shadowlines. However, unlike the northeast case, these shadowlines sometimes cross (as illustrated in Figure 3.1(b)–(d) and Figure 3.2(a)):

Definition 3.3. Given a permutation $\sigma = \sigma_1\sigma_2 \cdots \sigma_n \in \mathfrak{S}_n$, the *southwest shadow diagram* $D_{SW}(\sigma)$ of σ consists of the southwest shadowlines $L'_1(\sigma), L'_2(\sigma), \dots, L'_k(\sigma)$ formed as follows:

- $L'_1(\sigma)$ is the shadowline for those lattice points $(x, y) \in \{(1, \sigma_1), (2, \sigma_2), \dots, (n, \sigma_n)\}$ such that $S_{SW}(x, y)$ does not contain any other lattice points (and hence does not completely contain the southwest shadow of any other lattice points).
- While at least one of the points $(1, \sigma_1), (2, \sigma_2), \dots, (n, \sigma_n)$ is not contained in the shadowlines $L'_1(\sigma), L'_2(\sigma), \dots, L'_j(\sigma)$, define $L'_{j+1}(\sigma)$ to be the shadowline for the points

$$(x, y) \in \{(i, \sigma_i) \mid (i, \sigma_i) \notin \bigcup_{k=1}^j L'_k(\sigma)\}$$

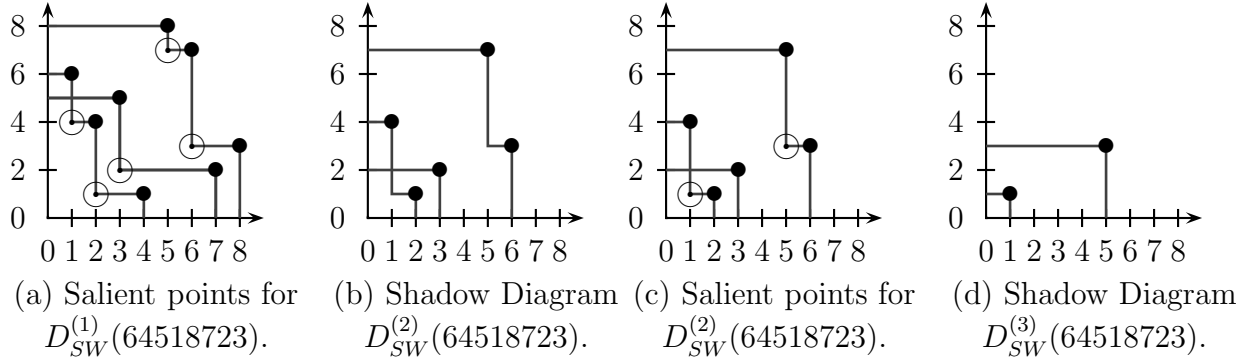


Figure 3.2: The southwest shadow diagrams for 64518723.

such that $S_{SW}(x, y)$ does not contain any other lattice points in the same set (and hence does not completely contain the southwest shadow of any of those points).

In other words, we again define a shadow diagram by recursively eliminating certain points in the permutation diagram until every point has been used to define a shadowline. However, we are here reversing both the direction of the shadows and the shadow containment property from the northeast case. It is in this sense that the geometric form for the Extended Patience Sorting Algorithm given in the next section can be viewed as “dual” to Viennot’s geometric form for RSK.

3.2 The Geometric Patience Sorting Algorithm

As in Section 2.2, one can produce a sequence $D_{SW}(\sigma) = D_{SW}^{(1)}(\sigma), D_{SW}^{(2)}(\sigma), \dots$, of shadow diagrams for a given permutation $\sigma \in \mathfrak{S}_n$ by recursively applying Definition 3.3 to salient points, with the restriction that new shadowlines can only connect points that were on the same shadowline in the previous iteration. (This reason for this important distinction from Geometric RSK is discussed further in Sections 4 and 5 below.) The salient points in this case are then naturally defined to be the southwest corner points of a given set of shadowlines. See Figure 3.2 for an example of how this works for the permutation in Example 1.3.

Moreover, the resulting sequence of shadow diagrams can then be used to reconstruct the pair of pile configurations given by the Extended Patience Sorting Algorithm (Algorithm 1.2). To accomplish this, index the cards in a pile configuration using the French convention for tableaux so that the row index increases from bottom to top and the column index from left to right. (In other words, we are labelling boxes as we would lattice points in the first quadrant of \mathbb{R}^2). Then, for a given permutation $\sigma \in \mathfrak{S}_n$, the elements of the i th row of the insertion piles $R(\sigma)$ (resp. recording piles $S(\sigma)$) are given by the largest ordinates (resp. abscissae) of the shadowlines that compose $D_{SW}^{(i)}$.

The main difference between this process and Viennot’s Geometric RSK is that care must be taken to assemble each row in its proper order. Unlike the entries of a Young tableau, the elements in the rows of a pile configuration do not necessarily increase from

left to right, and they do not have to be contiguous. As such, the components of each row should be recorded in the order that the shadowlines are formed. The rows can then uniquely be assembled into a legal pile configuration since the elements in the columns of a pile configuration must both decrease (when read from bottom to top) and appear in the left-most pile possible.

The proof for this is along the same lines as that of Viennot’s geometric RSK in that the shadowlines produced by Definition 3.3 are a visual record for how cards are played atop each other under Algorithm 1.2. In particular, it should be clear that, given a permutation $\sigma \in \mathfrak{S}_n$, the shadowlines in both of the shadow diagrams $D_{SW}^{(1)}(\sigma)$ and $D_{NE}^{(1)}(\sigma)$ are defined by the same lattice points from the permutation diagram for σ . In [3] the points along a given northeast shadowline are shown to correspond exactly to the elements in some column of $R(\sigma)$ (as both correspond to one of the left-to-right minima subsequences of σ). Thus, by reading the lattice points in the permutation diagram in increasing order of their abscissae, one can uniquely reconstruct both the piles in $R(\sigma)$ and the exact order in which cards are added to these piles (which implicitly yields $S(\sigma)$). In this sense, both $D_{SW}^{(1)}(\sigma)$ and $D_{NE}^{(1)}(\sigma)$ encode the bottom rows of $R(\sigma)$ and $S(\sigma)$ as given by Algorithm 1.2.

It is then easy to see by induction that the salient points of $D_{SW}^{(k-1)}(\sigma)$ yield the k^{th} rows of $R(\sigma)$ and $S(\sigma)$, and so this gives the following

Theorem 3.4. *The process described above for creating a pair of pile configurations $(R'(\sigma), S'(\sigma))$ from the Geometric Patience Sorting construction yields the same pair of pile configurations $(R(\sigma), S(\sigma))$ as the Extended Patience Sorting Algorithm (Algorithm 1.2).*

Having given the above Geometric form for Algorithm 1.2, it is worth pointing out that—as with RSK—there are various natural generalizations of Extended Patience Sorting for more general combinatorial objects including words and lexicographic arrays. (See [6] for a description of such extensions of RSK.) Moreover, many of these generalization can still similarly be realized as non-recursive analogs for the forms of RSK that can be applied to such objects. In particular, the authors in [5] explore several such generalizations and develop geometric forms for them much like the one given in this section.

In the case of words, Aldous and Diaconis [1] have given two different generalizations for Patience Sorting based upon whether cards with equal value are played on top of each other or not. These are called the “ties allowed” and “ties forbidden” cases, respectively, and the usual RSK and dual RSK algorithms can be modeled to develop bijective versions of them. The geometric forms for the resulting algorithms as given in [5] can then be compared to Fulton’s “Matrix-Ball” Geometric RSK algorithm (as defined in [6]) just as we compare the Geometric Patience Sorting given in this section to Viennot’s Geometric RSK in Section 4.

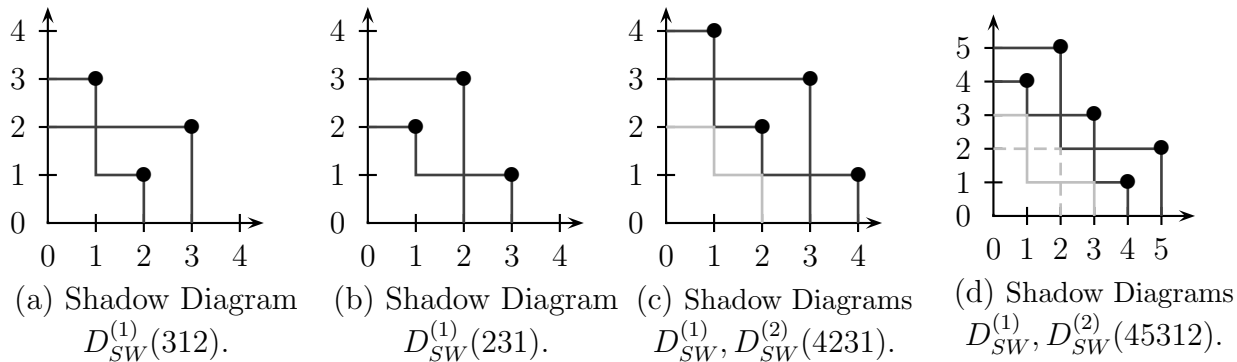


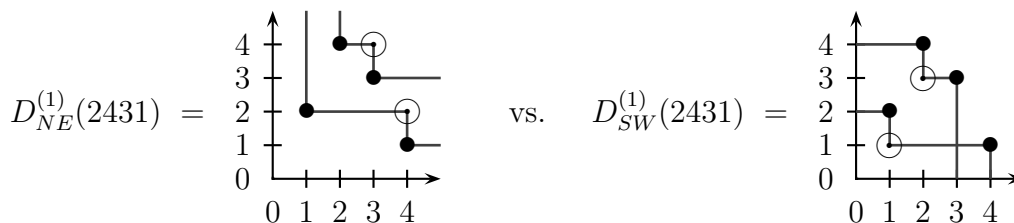
Figure 4.1: Shadow diagrams with different types of crossings.

4 Comparing Geometric Patience Sorting with Geometric RSK

Extended Patience Sorting (Algorithm 1.2) can be viewed as a “non-bumping” version of the RSK algorithm for permutations in that cards are permanently placed into piles and are covered by other cards rather than being displaced by them. It is in this sense that one of the main differences between their geometric algorithms lies in how and in what order the salient points of their respective shadow diagrams are determined. In particular, as playing a card atop a pre-existing pile under Patience Sorting is essentially like non-recursive Schensted Insertion, certain particularly egregious “double bumps” that occur under the Schensted Insertion Algorithm prove to be too complicated to be properly modelled by the “static insertions” of Patience Sorting.

At the same time, it is also easy to see that for a given $\sigma \in \mathfrak{S}_n$, the cards atop the piles in the pile configurations $R(\sigma)$ and $S(\sigma)$ (as given by Algorithm 1.2) are exactly the cards in the top rows of the RSK insertion tableau $P(\sigma)$ and recording tableau $Q(\sigma)$, respectively. Thus, this raises the question of when the remaining rows of $P(\sigma)$ and $Q(\sigma)$ can likewise be recovered from $R(\sigma)$ and $S(\sigma)$. While this appears to be directly related to the order in which salient points are read (as illustrated in Example 4.1 below), one would ultimately hope to characterize the answer in terms of generalized pattern avoidance similar to the description of reverse patience words for pile configurations (as discussed in Section 5 below).

Example 4.1. Consider the northeast and southwest shadow diagrams for $\sigma = 2431$:



In particular, note that the order in which the salient points are formed (when read from left to right) is reversed. Such reversals serve to illustrate the inherent philosophical differences between RSK and the Extended Patience Sorting Algorithm.

As was mentioned in Section 3.2 above, another fundamental difference between Geometric RSK and Geometric Patience Sorting is that the latter allows certain crossings to occur in the lattice paths formed during the same iteration of the algorithm. Given $\sigma \in \mathfrak{S}_n$, we can classify the basic types of crossings in $D_{SW}^{(1)}(\sigma)$ as follows: First note that each southwest shadowline in $D_{SW}^{(1)}(\sigma)$ corresponds to a pair of decreasing sequences of the same length, namely a column from the insertion piles $R(\sigma)$ and its corresponding column from the recording piles $S(\sigma)$. Then, given two different pairs of such columns in $R(\sigma)$ and $S(\sigma)$, the shadowline corresponding to the rightmost (resp. leftmost) pair—under the convention that new columns are always added to the right of all other columns in Algorithm 1.2—is called the *upper* (resp. *lower*) shadowline. We then call a crossing of two shadowlines *horizontal* (resp. *vertical*) if it involves a horizontal (resp. vertical) segment of the upper shadowline.

We illustrate such crossings in the following example. In particular, note that the smallest examples of permutations with crossing southwest shadowlines are 312 and 231 since permutations of length two can clearly never have crossings in their southwest shadow diagrams. Moreover, a general characterization for the crossings illustrated in the example is given in [4].

Example 4.2.

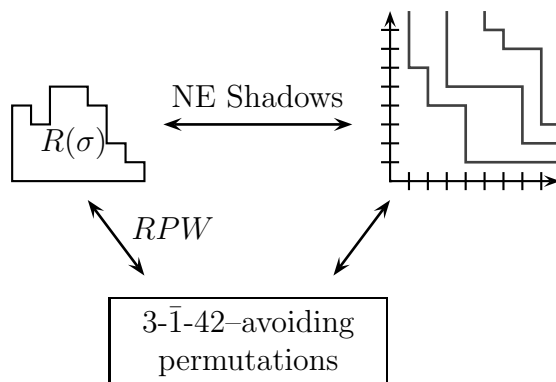
1. The smallest permutation for which $D_{SW}^{(1)}(\sigma)$ contains a horizontal crossing is $\sigma = 312$ as illustrated in Figure 4.1(a). The upper shadowline involved in this crossing is the one with only two segments.
2. The smallest permutation for which $D_{SW}^{(1)}(\sigma)$ contains a vertical crossing is $\sigma = 231$ as illustrated in Figure 4.1(b). As in part (1), the upper shadowline involved in this crossing is again the one with only two segments.
3. Consider $\sigma = 4231$. From Figure 4.1(c), $D_{SW}^{(1)}(\sigma)$ contains exactly two southwest shadowlines, and these shadowlines form a horizontal crossing followed by a vertical crossing. We call a configuration like this a “polygonal crossing.” Note in particular that $D_{SW}^{(2)}(\sigma)$ (trivially) has no crossings.
4. Consider $\sigma = 45312$. From Figure 4.1(d), $D_{SW}^{(1)}(\sigma)$ not only has a “polygonal crossing” (this time as two shadowlines have a vertical crossing followed by a horizontal one) but $D_{SW}^{(2)}(\sigma)$ does as well.

We further discuss “polygonal crossings” and their significance in Section 5 below.

We conclude this section by remarking again that, unlike the rows of Young tableaux, the values in the rows of a pile configuration do not necessarily increase when read from left to right. In fact, the descents in the rows of pile configurations are very closely related to the crossings given by Geometric Patience Sorting. For example, in [4], the authors prove that permutations for which no shadowlines at any iteration of Geometric Patience Sorting have crossings correspond exactly to so-called “stable pairs” of pile configurations (defined in Section 5) having the property that the rows in these pile configurations increase in value from left to right. Horizontal and vertical crossings are also characterized using barred permutation patterns in [4].

5 Geometric Patience Sorting and Generalized Permutation Patterns

In [3] the authors use northeast shadow diagrams to establish the following bijections for given $\sigma \in \mathfrak{S}_n$:



Note in particular that the lattice paths involved are not allowed to cross due to the shadow containment property used to define them in Section 2.1 above. This property and these bijections together give a nice characterization of when two permutations $\sigma, \tau \in \mathfrak{S}_n$ have the same pile configuration $R(\sigma) = R(\tau)$. In particular, we have the following theorem (first proven in [3]):

Theorem 5.1. *Let $\sigma, \tau \in \mathfrak{S}_n$. Then σ and τ have the same pile configurations under Patience Sorting if and only if there exists a sequence of 3-1-42 to 3-1-24 interchanges (equivalently, a sequence of changing 2-31 patterns into 2-13 patterns such that no 2-31 pattern is contained in an occurrence of a 3-1-42 pattern) that transform σ into τ .*

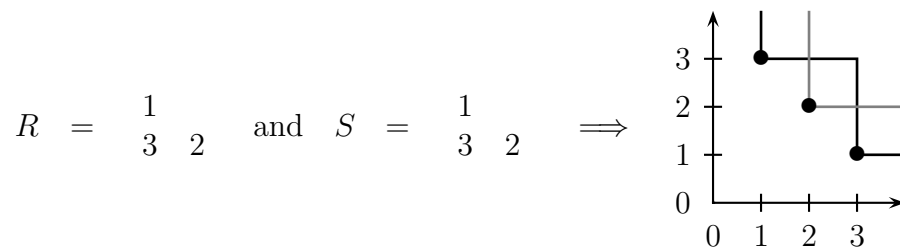
Consequently, northeast shadow diagrams suffice in geometrically characterizing the set $S_n(3\bar{1}\text{-}42)$ of 3-1-42-avoiding permutations (i.e., those avoiding the generalized pattern 2-31 unless its instance is contained in an instance of 3-1-42 pattern).

In [3] the authors also prove the following theorem using northeast shadow diagrams:

Theorem 5.2. *Extended Patience Sorting (Algorithm 1.2) gives a bijection between the symmetric group \mathfrak{S}_n and ordered pairs (σ, τ) of $3\bar{1}42$ -avoiding permutations such that σ if contains a $31\text{-}2$ pattern as a subword ω , then τ avoids a $13\text{-}2$ patterns in the subword whose elements have the same positions in τ as ω does in σ .*

A geometric explanation for this bijection in terms of northeast shadow diagrams involves the following example (which also explains our usage of the term “stable pairs” for those pairs of permutations (σ, τ) satisfying the theorem):

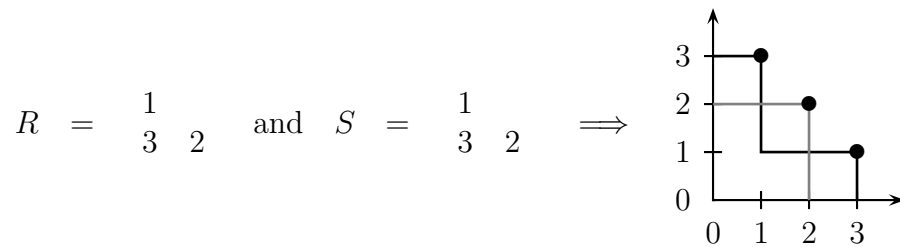
Example 5.3. Define the pile configuration $R = \{\{3 > 1\}, \{2\}\}$ (which corresponds to the $3\bar{1}42$ -avoiding permutation 312 under Theorem 5.1), and try constructing the pre-image of the pair $(R, S) = (R, R)$ under Algorithm 1.2 as follows:



In particular, starting with the lattice points $\{(1, 3), (2, 2), (3, 1)\}$ as given by the pair of pile configurations (values in R specify ordinates and values in S the abscissae; see [3]), we have superimposed the shadow diagram corresponding to the columns of R onto them. These two competing constructions then result in (R, S) being an “unstable pair” of pile configurations in that they yield intersecting northeast shadowlines under this inverse construction.

Recall from Section 3.1, however, that southwest shadow diagrams are allowed to cross in general. As such, while Geometric Patience Sorting allows us to geometrically characterize the bijection given in Theorem 5.2, the interpretation involves a much closer look at the crossings that result from trying to arbitrarily invert Algorithm 1.2. We illustrate this in the following example.

Example 5.4. As in Example 5.3, let $R = \{\{3 > 1\}, \{2\}\}$, and again try constructing the pre-image of the pair $(R, S) = (R, R)$ under Algorithm 1.2 as follows:



Again, we have started with the lattice points $\{(1, 3), (2, 2), (3, 1)\}$ as given by the pair of pile configurations and have superimposed the shadow diagram corresponding to the columns of R onto them. These two competing constructions then result in (R, S) being an “unstable pair” of pile configurations for a much deeper reason than just the resulting intersection in these southwest shadowlines. Here, the permutation 312 given by the entries in the pair (R, S) is a reverse patience word, and so, as proven in [4], its southwest shadow diagram should then avoid the so-called “polygonal crossing” that results. As such, we call the resulting shadow diagram “unstably crossing”.

Such polygonal crossings are what make it necessary to read only the salient points along the same shadowline in the order in which shadowlines are formed (as opposed to constructing the subsequent shadowlines using the entire partial permutation of salient points as in Viennot’s Geometric RSK). The reason for this is that further iterations of Geometric Patience Sorting for polygonally crossing shadowlines can contain “unstable pairs” as in the following example.

Example 5.5. Consider the shadow diagram of $\sigma = 45312$. The original shadowlines contain a polygonal crossing, and their iterates form an unstable pair as illustrated in Figure 4.1(d).

We conclude by stating a Schützenberger-type symmetry for Algorithm 1.2 that, while originally proven in [3], is now immediate from the Geometric Patience Sorting construction given in Section 3.2 (as both interchanging $R(\sigma)$ with $S(\sigma)$ and inverting σ are equivalent to reflecting the permutation diagram through the line $y = x$):

Theorem 5.6. *Let $(R(\sigma), S(\sigma))$ be the insertion and recording piles, respectively, formed by applying Algorithm 1.2 to $\sigma \in \mathfrak{S}_n$. Then reversing Algorithm 1.2 for $(S(\sigma), R(\sigma))$ yields the inverse permutation σ^{-1} .*

In [3] the authors remarked how Theorem 5.6 suggests that Algorithm 1.2 is the right generalization of normal Patience Sorting since it shares this same symmetry property with RSK applied to permutations. This point of view is now significantly strengthened by the Geometric characterization given for Algorithm 1.2 in Section 3.2 and the immediacy of this symmetry property from it. Moreover, the point of view of southwest shadow diagrams allows us to geometrically characterize the “stable pairs” of pile configurations resulting from this generalization (or equivalently certain pairs of 3- $\bar{1}$ -42-avoiding permutations by Theorem 5.2) whereas northeast shadow diagrams only really afford a direct geometric characterization of the 3- $\bar{1}$ -42-avoiding permutations involved.

References

- [1] D. Aldous and P. Diaconis. “Longest Increasing Subsequences: From Patience Sorting to the Baik-Deift-Johansson Theorem”, *Bull. Amer. Math. Soc.* **36** (1999), 413–432. Available online at <http://www.ams.org/bull/1999-36-04/>

- [2] M. Bóna. *Combinatorics of Permutations*. Chapman & Hall/CRC Press, 2004.
- [3] A. Burstein and I. Lankham. “Combinatorics of Patience Sorting Piles”. *Proceedings of Formal Power Series and Algebraic Combinatorics* (FPSAC 2005), June 2005, Taormina, Italy.
- [4] A. Burstein and I. Lankham. “Non-intersecting Patience Sorting Shadow Diagrams and Barred Permutation Patterns.” In preparation.
- [5] A. Burstein and I. Lankham. “Patience Sorting on Words and Lexicographic Arrays.” In preparation.
- [6] W. Fulton. *Young Tableaux*. LMS Student Texts 35. Cambridge University Press, 1997.
- [7] C. L. Mallows. “Problem 62-2, Patience Sorting”. *SIAM Review* **4** (1962), 148–149.
- [8] C. L. Mallows. “Problem 62-2”. *SIAM Review* **5** (1963), 375–376.
- [9] B. Sagan. *The Symmetric Group, Second Edition*. Graduate Texts in Mathematics 203. Springer-Verlag, 2000.
- [10] G. Viennot. “Une forme géométrique de la correspondance de Robinson-Schensted”, in *Combinatoire et Représentation du Groupe Symétrique*, D. Foata, ed. Lecture Notes in Mathematics 579. Springer-Verlag, 1977, pp. 29–58.